Rpe65 is necessary for production of 11-*cis*-vitamin A in the retinal visual cycle

T. Michael Redmond[1], Shirley Yu[1], Eric Lee[2], Dean Bok[3], Duco Hamasaki[4], Ning Chen[5], Patrice Goletz[5], Jian-Xing Ma[5], Rosalie K. Crouch[5] & Karl Pfeifer[2]

Mutation of *RPE65* can cause severe blindness from birth or early childhood, and RPE65 protein is associated with retinal pigment epithelium (RPE) vitamin A metabolism. Here, we show that *Rpe65*-deficient mice exhibit changes in retinal physiology and biochemistry. Outer segment discs of rod photoreceptors in *Rpe65*$^{-/-}$ mice are disorganized compared with those of *Rpe65*$^{+/+}$ and *Rpe65*$^{+/-}$ mice. Rod function, as measured by electroretinography, is abolished in *Rpe65*$^{-/-}$ mice, although cone function remains. *Rpe65*$^{-/-}$ mice lack rhodopsin, but not opsin apoprotein. Furthermore, all-*trans*-retinyl esters over-accumulate in the RPE of *Rpe65*$^{-/-}$ mice, whereas 11-*cis*-retinyl esters are absent. Disruption of the RPE-based metabolism of all-*trans*-retinyl esters to 11-*cis*-retinal thus appears to underlie the *Rpe65*$^{-/-}$ phenotype, although cone pigment regeneration may be dependent on a separate pathway.

Introduction

RPE65, a protein preferentially and abundantly expressed in the RPE (ref. 1), is essential for the maintenance of normal vision. Mutations in *RPE65* result in severe forms of early-onset retinal dystrophy, including Leber congenital amaurosis (LCA; OMIM 180069 and 204100; http://www.ncbi.nlm.nih.gov/Omim) and autosomal recessive, childhood-onset severe retinal dystrophy[2–5] (arCSRD). Mutations in this gene may account for 15% of cases of LCA, a genetically heterogeneous disorder, in North America[5]. *RPE65* has been localized to human chromosome 1p31 (refs 6,7) and its mouse homologue (*Rpe65*) to distal mouse chromosome 3 (ref. 6). By linkage analysis, certain arCSRDs were localized to the interval occupied by *RPE65* and were shown to be associated with mutations in *RPE65* (ref. 3). In addition, candidate gene analysis of *RPE65* identified mutations in patients with LCA (ref. 4,5). Common features of these patients include loss of vision from birth or early childhood associated with complete night-blindness, extinguished rod electroretinography and severely compromised cone responses, all suggestive of a role for RPE65 in retinal function.

Although the precise function of RPE65 is not known, a role in vitamin A metabolism is suspected[2,8,9]. Evidence for this is provided by its biochemical association with retinol-binding protein[9] (RBP) and 11-*cis*-retinol dehydrogenase[10]. RPE65, also known as p63 (ref. 9), has been proposed to be the RPE RBP receptor[9]. Association with 11-*cis*-retinol dehydrogenase suggests that RPE65 is part of the visual cycle pathway, the process by which the 11-*cis*-retinal chromophore of visual pigments is photo-isomerized to the all-*trans*-isomer, which is then regenerated in the dark[11,12]. The chromophore of mammalian opsins, 11-*cis*-retinal, is restricted to the eye. In the vertebrate eye, the major site of production of 11-*cis*-retinoids is the RPE (refs 13,14). The molecular identity of the retinoid isomerase or isomerohydrolase, despite years of study, is still unknown[15].

In view of the potentially important role of RPE65 in the physiology of vision and perhaps the visual cycle, we generated a targeted disruption of mouse *Rpe65*, as a natural mouse mutation is not known. In parallel with the human diseases described above, mutant mice showed severe changes in visual function. This may be related to supply of the 11-*cis*-retinal chromophore, as rhodopsin was absent from *Rpe65*-deficient mice, although opsin was present. These changes were restricted to the rod photoreceptors, leaving cones relatively unaffected.

Results

Disruption of mouse *Rpe65*

We designed a gene targeting protocol for the disruption of mouse *Rpe65* that replaced a 5′ region containing 1.1 kb of 5′ flanking region, exons 1, 2 and 3, intervening introns and 0.5 kb of intron c with the PGK-neo gene (Fig. 1*a*), along with loss of a *Hin*dIII site. *Rpe65*$^{+/+}$ mice showed only the 4.9-kb *Hin*dIII fragment on Southern-blot analysis and *Rpe65*$^{-/-}$ only the mutant 5.9-kb *Hin*dIII fragment, whereas *Rpe65*$^{+/-}$ progeny had a single copy of each (Fig. 1*b*). A normal mendelian distribution of genotypes was observed, indicating no effect of the mutation on viability. To confirm that transcription of *Rpe65* was disrupted in *Rpe65*$^{-/-}$ mice, RT-PCR was performed on total RNA isolated from whole mouse eyes. No *Rpe65* RT-PCR product was seen in *Rpe65*$^{-/-}$ mice, although the *Gapd* control transcript was amplified (Fig. 1*c*). As the *Rpe65* transcript region amplified was downstream of the disruption (exons 4–6), supernumerary transcription of a 5′-truncated mutant mRNA could be discounted.

Subtle photoreceptor changes in *Rpe65*$^{-/-}$ mice

By light microscopy, changes in the RPE of 7-week-old and 15-week-old *Rpe65*$^{-/-}$ mice were minimal compared with *Rpe65*$^{+/+}$ or *Rpe65*$^{+/-}$ littermates (Fig. 2), although in *Rpe65*$^{-/-}$ animals there were subtle and slowly progressing changes in the pho-

[1]*Laboratory of Retinal Cell and Molecular Biology, National Eye Institute and* [2]*Laboratory of Mammalian Genes and Development, National Institute of Child Health and Human Development, National Institutes of Health, Bethesda, Maryland 20892, USA.* [3]*Jules Stein Eye Institute, Brain Research Institute and Department of Neurobiology, UCLA School of Medicine, Los Angeles, California 90095, USA.* [4]*Bascom-Palmer Eye Institute, University of Miami School of Medicine, Miami, Florida 33101, USA.* [5]*Storm Eye Institute, Medical University of South Carolina, Charleston, South Carolina 29425, USA. Correspondence should be addressed to T.M.R. (e-mail: redmond@helix.nih.gov).*

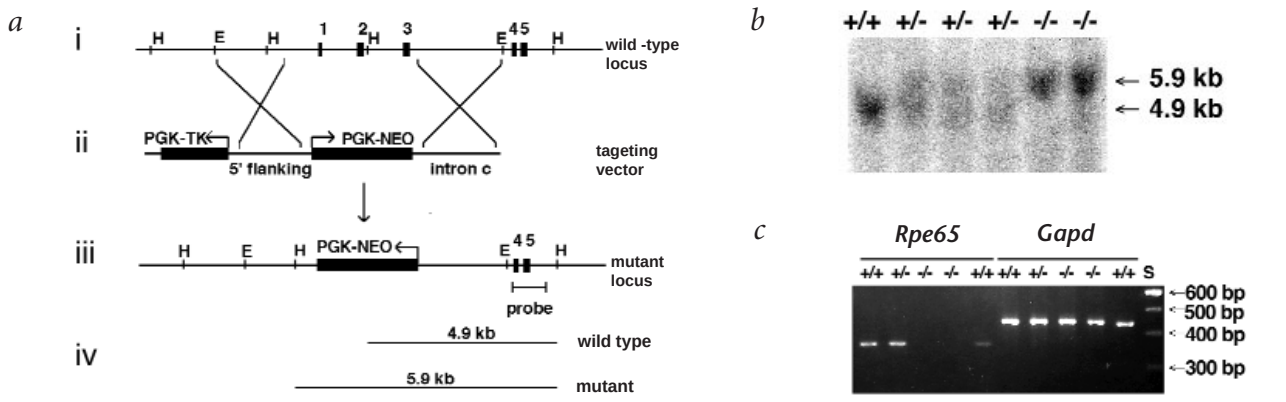

Fig. 1 Targeted disruption of the *Rpe65* locus. ***a***, Strategy: (i), 5′ end of wild-type *Rpe65*; (ii), targeting vector; (iii), targeted locus; (iv), sizes of *Hin*dIII fragments from wild-type and mutant loci, respectively, hybridized to probe indicated in (iii). H, *Hin*dIII sites; E, *Eco*RI restriction sites. ***b***, Southern-blot analysis of genomic DNA from progeny of a heterozygous cross digested with *Hin*dIII, using a flanking probe showing wild-type (4.9 kb) and/or mutant (5.9 kb) *Hin*dIII restriction fragments (*a*, iv). ***c***, RT-PCR analysis of *Rpe65* mRNA expression in progeny of a heterozygous cross. The left set of lanes are results of *Rpe65*-specific RT-PCR on cDNA reverse transcribed from total RNA of whole eyes from *Rpe65*$^{+/-}$, *Rpe65*$^{-/-}$ and *Rpe65*$^{+/+}$ mice, whereas the right set are results of *Gapd*-specific RT-PCR on the same cDNA. The *Rpe65* mRNA-specific, 366-bp band is absent from *Rpe65*$^{-/-}$, whereas the *Gapd*-specific 452-bp band is present; S, 100-bp ReadyLoad DNA Ladder.

toreceptor cells. No differences were seen between *Rpe65*$^{+/+}$ and *Rpe65*$^{+/-}$ littermates. At seven weeks of age, the outer segment (OS) region of *Rpe65*$^{-/-}$ photoreceptors stained less densely with toluidine blue than did those of *Rpe65*$^{+/+}$ or *Rpe65*$^{+/-}$ littermates (Fig. 2*a*–*c*). This could be interpreted as loss of, or less dense packing of, OS discs. This was more evident by 15 weeks (Fig. 2*d*,*e*), by which time the length of the outer segments was significantly decreased in *Rpe65*$^{-/-}$ mice and more voids were seen, consistent with loss of OS material. A slow degeneration was also seen with loss of photoreceptor nuclei. In 7-week-old and 15-week-old *Rpe65*$^{+/+}$ and *Rpe65*$^{+/-}$ mouse retinae, there were 10–11 layers of nuclei (Fig. 2*a*,*b*,*d*), comparable with retina from 7-week-old *Rpe65*$^{-/-}$ retina (Fig. 2*c*). By 15 weeks of age, the number of nuclear layers had decreased to 8–9 (Fig. 2*e*) in *Rpe65*$^{-/-}$ retina, and by 28 weeks to 7 (data not shown).

By electron microscopy (EM), the OS of rod photoreceptors appear to be slightly altered at seven weeks of age compared with those of wild type (Fig. 3*a*,*b*). Rod photoreceptor OS discs in *Rpe65*$^{-/-}$ mice are not as tightly packed as in *Rpe65*$^{+/+}$ and *Rpe65*$^{+/-}$ littermates, resulting in more apparent voids in the sections. This feature contributes to the more disorganized appearance of these *Rpe65*$^{-/-}$ OS (Fig. 3*a*,*b*). The *Rpe65*$^{-/-}$ OS were also shorter in length than those of wild type. At 15 weeks of age, the OS of *Rpe65*$^{-/-}$ mice were more disorganized than at 7 weeks (Fig. 2*e*, and data not shown). OS morphogenesis thus appears to be subtly affected initially by *Rpe65*-deficiency in the RPE; OS discs are elaborated and deployed, as in wild type, although they are not as regularly packed. In older animals the level of disorganization increases. Alterations in OS phagocytosis by the RPE were not evident. In the RPE of

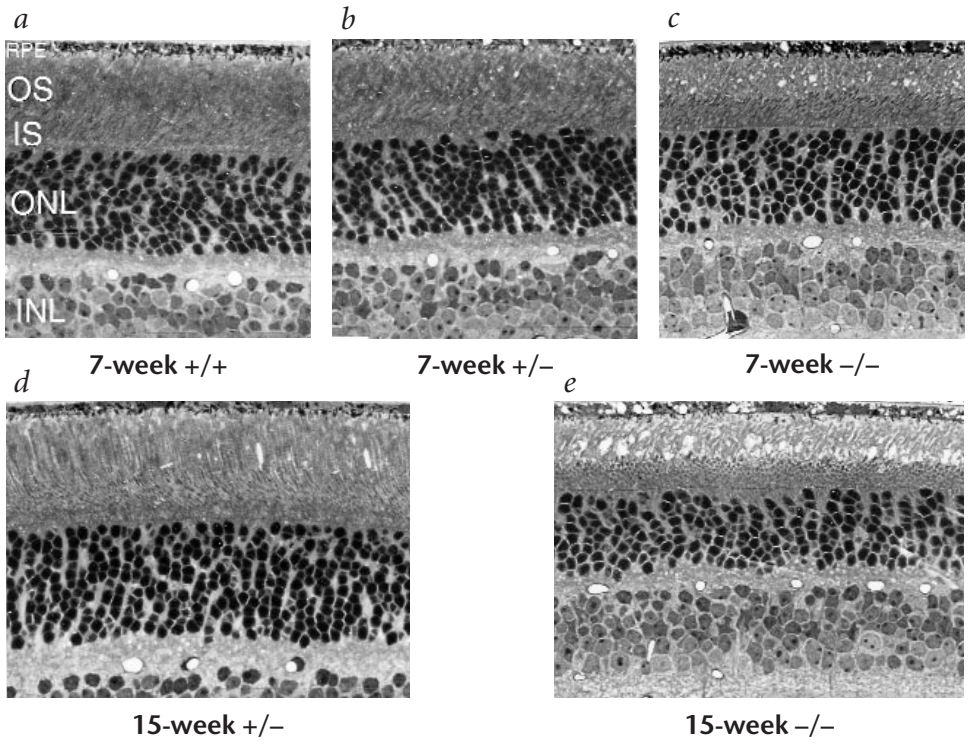

Fig. 2 Light micrographs of *Rpe65*$^{+/+}$, *Rpe65*$^{+/-}$ and *Rpe65*$^{-/-}$ mice. Seven-week-old *Rpe65*$^{+/+}$ (***a***), 7-week-old *Rpe65*$^{+/-}$ (***b***), 7-week-old *Rpe65*$^{-/-}$ (***c***), 15-week-old *Rpe65*$^{+/-}$ (***d***) and 15-week-old *Rpe65*$^{-/-}$ (***e***) mice are shown. Retinal pigment epithelium, RPE; rod outer segments, OS; rod inner segments, IS; photoreceptor outer nuclear layer, ONL; inner nuclear layer, INL.

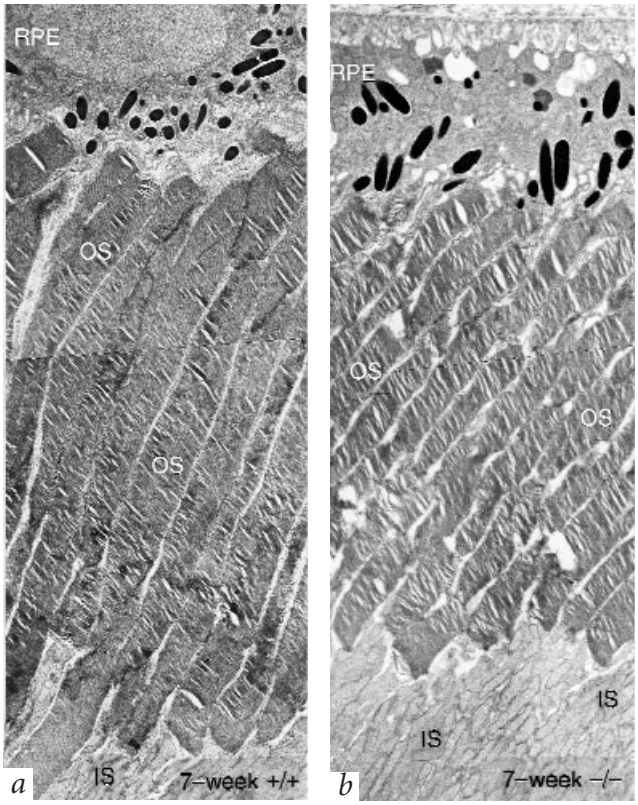

Fig. 3 Electron microscopy of outer retina of *Rpe65*-deficient and normal mice. Seven-week-old *Rpe65*$^{+/+}$ (***a***) and 7-week-old *Rpe65*$^{-/-}$ (***b***) mice are shown. Retinal pigment epithelium, RPE; rod outer segments, OS; rod inner segments, IS.

15-week-old *Rpe65*$^{-/-}$ mice, numerous lipid inclusions were also present (Fig. 8*d*).

No gross changes were seen in tissues or organs outside the eye. To address the possibility that a generalized systemic effect on vitamin A-requiring organs occurred, other organs containing retinol-dependent cells, including kidney and testis, were analysed for histological changes. No differences were observed in *Rpe65*$^{-/-}$ mice when compared with *Rpe65*$^{+/+}$ or *Rpe65*$^{+/-}$ littermates (data not shown).

Rod photoreceptor ERG is abolished in *Rpe65*$^{-/-}$ mice

The electroretinograms (ERGs) recorded from dark-adapted *Rpe65*$^{+/+}$ and *Rpe65*$^{+/-}$ mice were typical of ERG responses recorded from other strains of normal mice with normal a-, b- and c-waves. The dark-adapted ERG responses of the *Rpe65*$^{-/-}$ mice on the other hand were very different; the a-wave was very small, the c-wave was not evident and the b-wave was small and had fast rising and falling limbs. The mean and standard error of the mean of the b-wave amplitude for *Rpe65*$^{+/+}$, *Rpe65*$^{+/-}$ and *Rpe65*$^{+/-}$ mice are shown (Fig. 4). The full intensity stimulus was reduced by use of neutral density (ND) filters. For both *Rpe65*$^{+/+}$ and *Rpe65*$^{+/-}$ mice, a small (20–30 μV) b-wave was elicited by a stimulus of ND=6.0 (1.59×10^{-3} cd/m^2). Further increases in the stimulus intensity increased the b-wave amplitude until it saturated at a stimulus intensity of ND=3.0 (1.59 cd/m^2). Additional increases in the stimulus intensity did not change the amplitude until the stimulus intensity was ND=2.0 (1.59×10 cd/m^2) when the photopic segment of the b-wave was evoked. The mean of the maximum b-wave amplitude was 960.0 μV for *Rpe65*$^{+/+}$ and 937.6 μV for *Rpe65*$^{+/-}$ mice. The mean intensity:response curves for these mice did not differ significantly and resembled the curves reported previously for mice and other animals. The mean intensity:response curve for *Rpe65*$^{-/-}$ mice was very different; the curve was displaced to higher intensities by approximately 4.5 log units, and the maximum b-wave amplitude was 256.0 μV. Thus, there is a very reduced dark-adapted ERG response in *Rpe65*-deficient mice; although there is a response to high intensity light. In the mouse, as in other animals, the ERG response in the dark-adapted state is mostly due to rod activity, however, under bright light conditions, rod activity is suppressed and only the cone pathway contributes to the ERG (ref. 16).

Next, ERG responses were recorded under light-adapted or photopic conditions by increasing stimulus intensities in the dark, and then with increasing levels of steady background illumination (Fig. 5*a*). In 14-week-old *Rpe65*$^{+/+}$ mice in the dark (No Bkgd), the amplitude of the b-wave increased (Fig. 4). With an ND=6.0 steady background illumination, the intensity:response curve was shifted to the right (higher intensities) by approximately 0.8 log units, and the b-wave amplitude increased. Further increases in the background intensity shifted the curve further to the right. Similar data were obtained from heterozygous mice (data not shown). In 14-week-old *Rpe65*$^{-/-}$ animals, however, the intensity:response curves for the eye in the dark, and with background intensities of ND=4.0, 3.0 and 2.0, were approximately the same. These findings suggest that the ERG responses of *Rpe65*$^{-/-}$ mice are cone-driven; a plot of the mean intensity:response curve for the *Rpe65*$^{+/+}$ mouse with a ND=2.0 background intensity was not significantly different from that of the *Rpe65*$^{-/-}$ mouse obtained in the dark (data not shown). Further demonstration that the ERGs from *Rpe65*$^{-/-}$ mice are cone-driven comes from the shapes of the ERGs. The shape of the ERG responses of the *Rpe65*$^{-/-}$ mouse elicited by the full intensity stimulus in the dark closely resembles the photopic ERG responses of the *Rpe65*$^{+/+}$ mouse with a –2.0 background (Fig. 5*b*, inset) and photopic ERGs previously reported for mice. Additional evidence that the ERG responses of the *Rpe65*-deficient mouse were cone-driven came from flicker testing. Two *Rpe65*$^{-/-}$ mice responded only to high frequency flicker (in the cone response range) and only at higher stimulus intensities, whereas *Rpe65*$^{+/+}$ and *Rpe65*$^{+/-}$ mice responded to low frequency flicker (rod range) only at low stimulus intensity and to all frequencies at high stimulus intensity, as expected.

Rhodopsin is absent from *Rpe65*$^{-/-}$ mouse retina

To better understand the total abrogation of rod ERG response, we analysed the rhodopsin status of dark-adapted *Rpe65*$^{-/-}$ mice

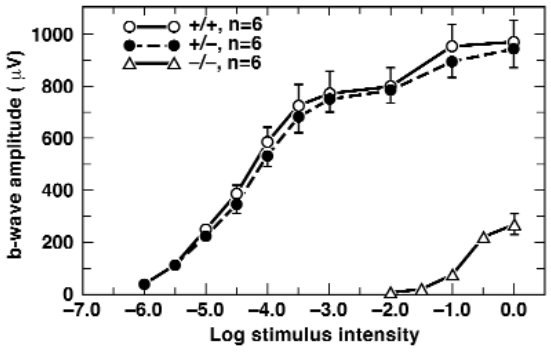

Fig. 4 Dark-adapted ERG responses in *Rpe65*-deficient mice. Intensity response curves for 6 *Rpe65*$^{+/+}$, 6 *Rpe65*$^{+/-}$ and 6 *Rpe65*$^{-/-}$ mice derived from ERGs recorded from 10-week-old *Rpe65*$^{+/+}$, *Rpe65*$^{+/-}$ and *Rpe65*$^{-/-}$ mice. Stimulus intensities are designated by the neutral density filters used to attenuate the full intensity (0) stimulus. At ND=0, luminance=1.59×10^3 cd/m^2. ERGs were recorded with DC-coupling. Stimulus duration=4.0 s. Mean and s.e.m. are shown.

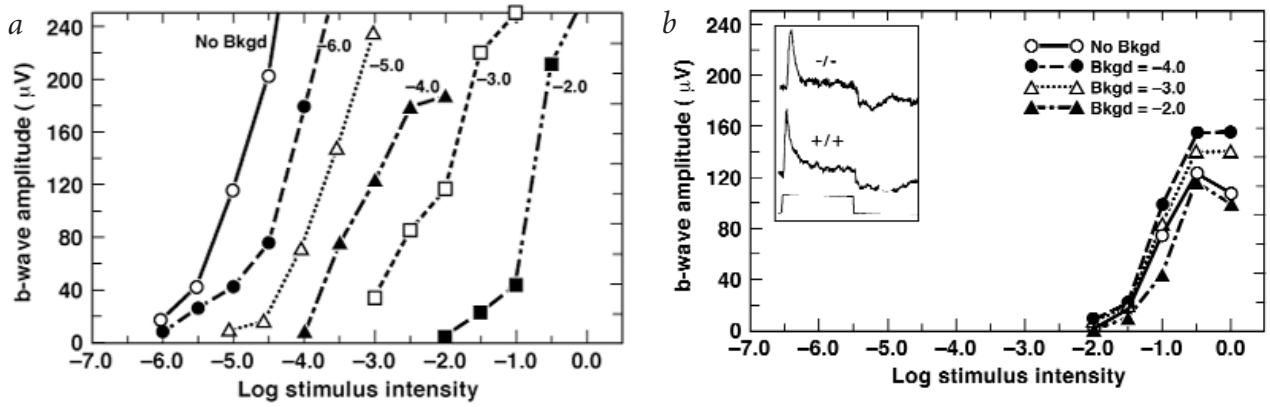

Fig. 5 Light-adapted ERG responses in *Rpe65*-deficient mouse. ***a***, Intensity-response curves obtained from a 14-week-old $Rpe65^{+/+}$ mouse. ERGs were recorded in the dark (No Bkgd) and with different background illumination. The intensity of the background illumination is designated by the neutral density (ND) filter used to attenuate the full intensity background. At ND=2.0, the background luminance was 5.52 cd/m^2. ***b***, Intensity-response curves obtained from a 14-week-old $Rpe65^{-/-}$ mouse. ERGs recorded as in (a). Inset shows the ERGs elicited by the full intensity stimulus from an $Rpe65^{-/-}$ mouse with no background illumination (top), and an $Rpe65^{+/+}$ mouse with an ND=2.0 background (bottom).

compared with $Rpe65^{+/+}$ or $Rpe65^{+/-}$ littermates (Fig. 6*a*). Total dark-adapted retina rhodopsin was detergent extracted and the unregenerated difference spectrum measured to assess endogenous rhodopsin. A typical rhodopsin absorption maximum was observed at 500 nm. Normal amounts of total rhodopsin were detergent extracted from $Rpe65^{+/+}$ mouse retina of different ages (Fig. 6*a*, trace A for a representative spectrum). Less rhodopsin was extractable from $Rpe65^{+/-}$ littermates (Fig. 6*a*, trace B for a representative spectrum), however, no rhodopsin was extractable from dark-adapted $Rpe65^{-/-}$ mice retina of different ages, as shown by the flat difference spectrum (Fig. 6*a*, trace C for a representative spectrum). When exogenous 11-*cis*-retinal chromophore was added to rhodopsin extracts, some regeneration of rhodopsin was seen in $Rpe65^{-/-}$ mouse extracts, as shown by the slight increase in the difference spectrum (Fig. 6*b*, trace C), indicating that at least a fraction of the opsin was structurally intact. Conversely, the limited increase suggests that much of the opsin is not able to be regenerated. Considering its relatively normal appearance in 7-week-old animals, morphogenesis of the $Rpe65^{-/-}$ OS does not appear to be affected by lack of rhodopsin.

As a further measure of photoreceptor function, apoprotein opsin was measured in $Rpe65^{-/-}$, $Rpe65^{+/+}$ and $Rpe65^{+/-}$ littermates. Opsin was detected by immunoblot in all three genotypes (Fig. 7*a*, top; $Rpe65^{+/+}$>$Rpe65^{+/-}$>$Rpe65^{-/-}$). The integrity of the photoreceptors was shown by immunoblot using an antibody to the α-subunit of transducin, $G_{\alpha t}$ (Fig. 7*a*, bottom). Opsin was located in the outer segments of the rod photoreceptors, the physiologically appropriate compartment, in $Rpe65^{+/-}$ (Fig. 7*b*) and in $Rpe65^{-/-}$ (Fig. 7*c*) mice, as shown by opsin immunoelectron microscopy.

All-*trans*-retinyl esters over-accumulate in $Rpe65^{-/-}$ RPE

To determine whether the evident lack of 11-*cis*-retinal in the rod photoreceptors was due to lack of uptake of vitamin A by the RPE, uptake of vitamin A but lack of transport from the RPE of 11-*cis*-retinal (resulting in accumulation of 11-*cis*-retinyl esters), or uptake of vitamin A but lack of synthesis of 11-*cis*-retinoids, we performed HPLC analysis of RPE retinoids extracted from $Rpe65^{+/+}$ (Fig. 8*a*) and $Rpe65^{-/-}$ (Fig. 8*b*) mice. There was an over-accumulation of total retinyl esters in 15-week-old $Rpe65^{-/-}$ mice. Accumulated esters in the $Rpe65^{-/-}$ RPE were found to be all-*trans*-retinyl ester by ester saponification (Fig. 8*b*, inset). No peak was detected at the mobility of authentic 11-*cis*-retinol standard (Fig. 8*b*, denoted by solid arrow). As expected, a much smaller all-*trans*-retinol peak was seen in $Rpe65^{+/+}$ samples (Fig. 8*a*, inset), but no 11-*cis*-retinol peak was detectable under the conditions used. As 11-*cis*-retinyl ester has been previously found to comprise only 5% of total retinyl ester in normal 13-week-old mouse RPE (ref. 17), lack of detection of 11-*cis*-retinol in saponified $Rpe65^{+/+}$ samples was expected given the small amount of retinyl ester present. Similarly, given the increased amount of retinyl ester in the $Rpe65^{-/-}$ RPE (Fig. 8*c*), if 11-*cis*-retinyl ester were present in the same relative 5% abundance, it should be detectable. On the basis of these data, however, we cannot exclude the possibility that very low levels of 11-*cis*-retinoids are present in the RPE of *Rpe65*-deficient mice. A minor amount of the 13-*cis*-isomer (Fig. 8*b*,

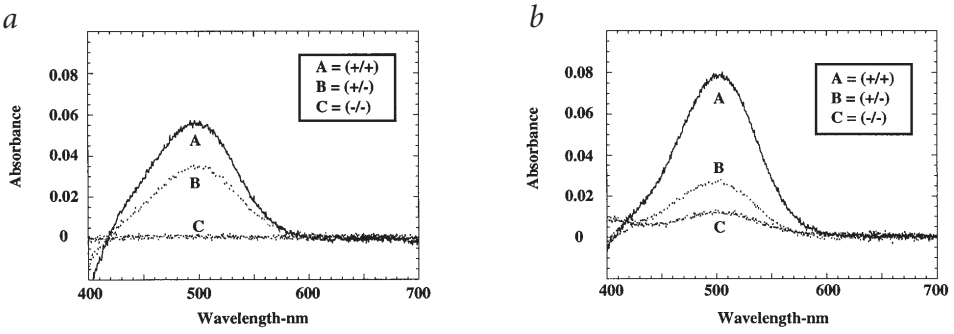

Fig. 6 Absence of holoprotein rhodopsin in *Rpe65*-deficient mouse retina. ***a***, Difference spectra of unregenerated rhodopsin extracted from 20-week-old $Rpe65^{+/+}$ (A), $Rpe65^{+/-}$ (B) and $Rpe65^{-/-}$ (C) littermates. Lack of absorption maximum at 500 nm in $Rpe65^{-/-}$ (C) trace indicates lack of endogenous rhodopsin. ***b***, Difference spectra of rhodopsin regenerated with exogenous 11-*cis*-retinal chromophore from 20-week-old $Rpe65^{+/+}$ (A), $Rpe65^{+/-}$ (B) and $Rpe65^{-/-}$ (C) littermates. Presence of absorption maximum at 500 nm in $Rpe65^{-/-}$ (C) trace indicates partial regenerability of residual opsin apoprotein in *Rpe65*-deficient retina.

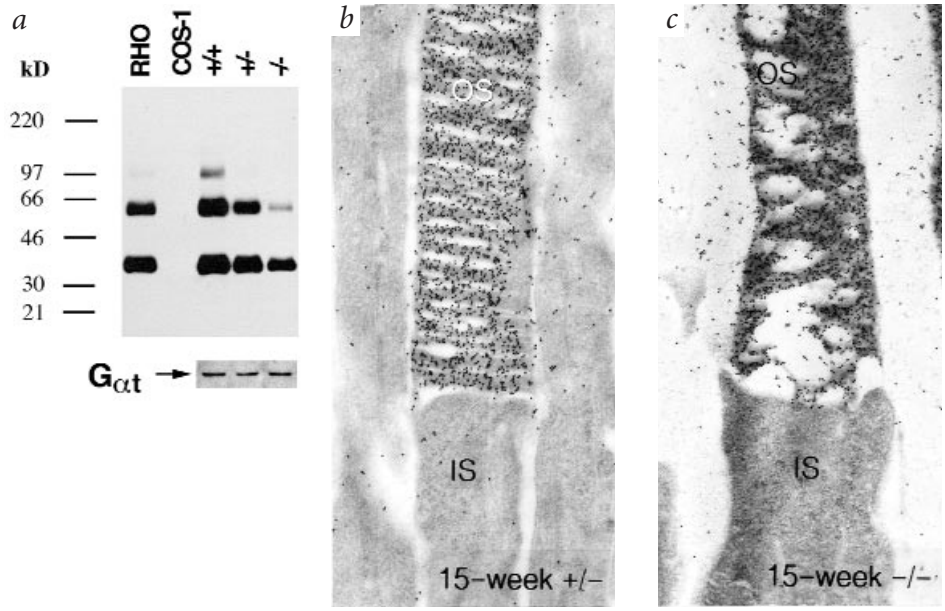

Fig. 7 Presence of apoprotein opsin in *Rpe65*-deficient mouse retina. ***a***, Top, immunoblot of retina protein extract from *Rpe65*$^{+/+}$, *Rpe65*$^{+/-}$ and *Rpe65*$^{-/-}$ mice compared with purified bovine rhodopsin (RHO; 5 ng) and COS-1 cell extract (50 ng). Primary antibody used was anti-rhodopsin monoclonal antibody 1D4 (ref. 48), which recognizes opsin apoprotein. The presence of monomeric, dimeric and trimeric rhodopsin is characteristic. Bottom, a control blot reacted with anti-transducin α-subunit ($G_{\alpha t}$) to confirm integrity of photoreceptor cells and equivalent loading. Immunoelectron microscopy of rod photoreceptor cells shows appropriate localization of opsin in rod outer segments (OS) in both *Rpe65*$^{+/-}$ (***b***) and *Rpe65*$^{-/-}$ (***c***) 15-week-old mice, and no evidence of abnormal accumulation in rod inner segments (IS). The apparent background staining to the left of the OS is due to displacement of opsin from these fragile structures during sectioning. Primary antibody used was anti-rhodopsin polyclonal antibody.

peak 1), derived from sample handling, was detected. This selective over-accumulation of all-*trans*-retinyl esters may be associated with morphological changes evident in the RPE of *Rpe65*$^{-/-}$ mice. A feature of the *Rpe65*$^{-/-}$ RPE at later ages, such as 15 weeks, is the presence of numerous inclusions visible at the electron microscope level (Fig. 8*d*) that appear to be lipid droplets. They range in form from electron-lucent to somewhat electron-opaque. This suggests that they contain lipid which has been partially or completely extracted by histological processing. In addition, 15-week-old *Rpe65*$^{-/-}$ RPE contained other unidentified structures with electron-translucent centers (Fig. 8*d*).

Discussion

The results presented here confirm the role of RPE65 in the vitamin A metabolism of the retina with the finding that the *Rpe65*-deficient mouse lacks rhodopsin, although it appropriately expresses the opsin apoprotein in the rod OS. This evident lack of 11-*cis*-retinal chromophore occurs alongside the over-accumulation of all-*trans*-retinyl esters in the RPE and implicates a block in the RPE visual cycle. At the same time, it appears that no 11-*cis*-retinyl ester accumulates. Although isomerohydrolase activity can be somewhat inhibited by 11-*cis*-retinol[14], storage of 11-*cis*-retinyl ester does occur in mouse RPE (ref. 17), given an active isomerization step. This concurrent lack of rhodopsin and over-accumulation of all-*trans*-retinyl ester (but apparently not of 11-*cis*-retinyl ester) in the *Rpe65*-deficient mouse RPE argues for a block in isomerization. Either one of these situations alone, unaccompanied by the other, would implicate a block in transport of retinoids, either into or out of the RPE into the photoreceptors. On the other hand, 11-*cis*-retinoids are, apparently, not com-

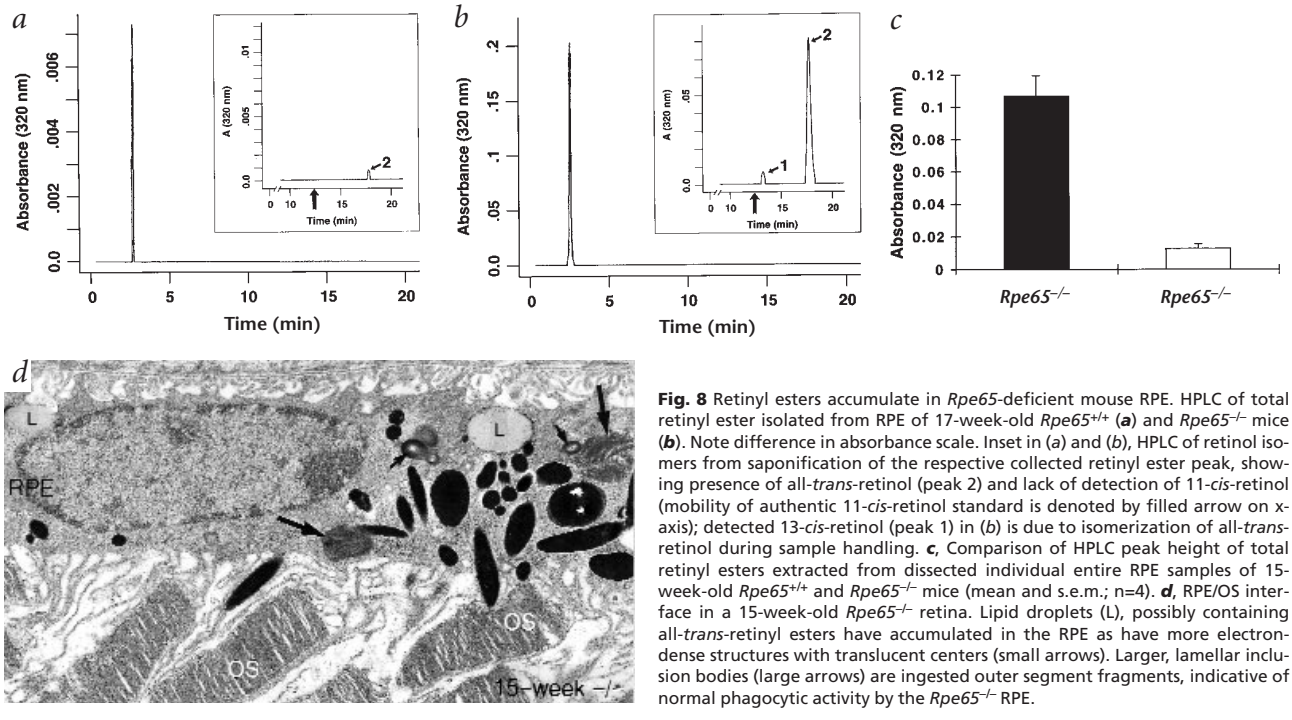

Fig. 8 Retinyl esters accumulate in *Rpe65*-deficient mouse RPE. HPLC of total retinyl ester isolated from RPE of 17-week-old *Rpe65*$^{+/+}$ (***a***) and *Rpe65*$^{-/-}$ mice (***b***). Note difference in absorbance scale. Inset in (*a*) and (*b*), HPLC of retinol isomers from saponification of the respective collected retinyl ester peak, showing presence of all-*trans*-retinol (peak 2) and lack of detection of 11-*cis*-retinol (mobility of authentic 11-*cis*-retinol standard is denoted by filled arrow on x-axis); detected 13-*cis*-retinol (peak 1) in (*b*) is due to isomerization of all-*trans*-retinol during sample handling. ***c***, Comparison of HPLC peak height of total retinyl esters extracted from dissected individual entire RPE samples of 15-week-old *Rpe65*$^{+/+}$ and *Rpe65*$^{-/-}$ mice (mean and s.e.m.; n=4). ***d***, RPE/OS interface in a 15-week-old *Rpe65*$^{-/-}$ retina. Lipid droplets (L), possibly containing all-*trans*-retinyl esters have accumulated in the RPE as have more electron-dense structures with translucent centers (small arrows). Larger, lamellar inclusion bodies (large arrows) are ingested outer segment fragments, indicative of normal phagocytic activity by the *Rpe65*$^{-/-}$ RPE.

pletely absent from *Rpe65*-deficient mouse retina, as cone photoreceptors are still functional, although the availability of this chromophore pool appears to be restricted to cones.

At the same time, our data argue against the hypothesis that RPE65 (ref. 9) is the RPE RBP receptor, because its absence does not prevent uptake of vitamin A by the RPE, although an RBP receptor has been identified in a variety of tissues, including the RPE, by binding studies[18–20]. Alternatively, cellular uptake of retinol by the RPE may be governed by the level of intracellular binding proteins (high in the RPE; ref. 21) and the rate of metabolism of vitamin A in target cells[22]. In the RPE of *Rpe65*-deficient mice, all-*trans*-retinol uptake is unimpaired, whereas over-accumulation of all-*trans*-retinyl esters may result in the RPE lipid inclusions in 15-week-old *Rpe65*-deficient mice, similar to those seen in the RPE of mice injected with all-*trans*-retinyl esters[23]. Retinyl esters also accumulate in the lipid droplets of frog RPE (ref. 24).

Although many components of the mammalian visual cycle have been characterized at the molecular level, including rhodopsin[25], interphotoreceptor retinoid-binding protein[26] (IRBP), ROS all-*trans*-retinol dehydrogenase[27], lecithin:retinol acyltransferase[28] (LRAT; which has been cloned; D.B., unpublished data), 11-*cis*-retinol dehydrogenase[10] and 11-*cis* specific cellular retinaldehyde-binding protein[29,30] (CRALBP), the all-*trans*: 11-*cis*-retinol isomerase or isomerohydrolase[13–15] remains incompletely characterized. Association of RPE65 with the putative 11-*cis*-retinoid-generating enzyme complex of the RPE is evident from its association with 11-*cis*-retinol dehydrogenase[9]. In addition, the first appearance of RPE65 (ref. 1) coincides with the first appearance of 11-*cis*-retinoids and retinol isomerase activity in the developing mouse and rat retina[17,31]. Our data indicate that metabolism of all-*trans*-retinyl ester to 11-*cis*-retinoid is blocked in the RPE in the absence of RPE65.

Rpe65-deficient mice are, in effect, functionally rhodopsin deficient. Although both *Rpe65*$^{-/-}$ and *Rho*$^{-/-}$ mice[32] lack rhodopsin, the morphological phenotypes expressed are distinct. In *Rpe65*$^{-/-}$ mice, rhodopsin holoprotein is not required for OS morphogenesis, whereas in *Rho*$^{-/-}$ mice, synthesis of opsin apoprotein is essential. Despite the presence of appropriately localized opsin in *Rpe65*$^{-/-}$ mouse retina, our results suggest that it may not be capable of regeneration. Although it may not be necessary for the initial synthesis of opsin, 11-*cis*-retinal may be required for its continued stability. Thus, chronic lack of chromophore may affect the ability of opsin to be regenerated in the OS. Further study of this possibility is required. Additionally, whereas both mutant mouse rod photoreceptors are non-functional, the OS-lacking *Rho*$^{-/-}$ photoreceptors degenerate far faster than OS-bearing *Rpe65*$^{-/-}$ photoreceptors[32].

A central feature of the *Rpe65*-deficient phenotype is the abolition of rod ERG responses. The OS of *Rpe65*$^{-/-}$ are well-preserved compared with the OS of *Rbp3*$^{-/-}$ mice, which have a rod ERG response, implying movement of retinoids despite lack of the transport protein[33]. Thus even when transport is impaired, some chromophore can still reach the photoreceptors. Although lowered levels of rhodopsin (and opsin) are seen in *Rpe65*$^{+/-}$ animals compared with *Rpe65*$^{+/+}$ animals, their OS morphology is identical and their ERG responses are normal, suggesting that rod photoreceptor cells have a wide range of tolerance for rhodopsin level. This is in agreement with similar findings in *Rho*$^{+/-}$ mice[32]. In contrast, cone ERG function in the *Rpe65*-deficient mice is preserved. This finding corroborates the conclusion that cone and rod pathways of regeneration may be different or separate[34]. These results suggest that two separate visual cycles may operate in the mammalian retina: one centred in the RPE supplying the rod photoreceptors and another supplying the cones. Cultured chicken Muller retinal glial cells have been shown to secrete 11-*cis*-retinol into media[35] and may play a role. Furthermore, mammalian cones, unlike rods, can resensitize with added 11-*cis*-retinol[36], and amphibian cones[34,37] and cone-like pigments[38] separated from the RPE can be regenerated. The recent identification of *RPE65*-like mRNA expression in cone, but not rod, photoreceptors of salamander is supportive of this[39].

The *Rpe65*-deficient mouse is the first *in vivo* evidence that a distinct mammalian cone-associated visual cycle, or mechanism of regeneration, may exist. This raises differences between the *Rpe65*$^{-/-}$ mouse and the human LCA phenotypes, as in the latter, both rod and cone function are abolished or severely compromised[3–5]. This may be due to the relative age at which ERGs are measured in mice and human patients, or from species-specific differences in retinal anatomy and cone distribution. Mice have two types of cone cells scattered throughout the retina, one a middle-wave (510 nm) cone and the other a short-wave (370 nm)–sensitive cone that may be homologous to the human blue cone[40]. In the human retina, red- and green-sensitive cone cells are concentrated in the central area of high cone density known as the fovea, whereas blue-sensitive cones are scattered throughout the retina[41]. Perhaps this very dense concentration of highly active cones is not amenable to supply by the associated Muller cells and is therefore dependent on the RPE for regeneration.

These *Rpe65*-deficient mice provide a model system to study potential therapies for human diseases caused by *RPE65* defects. RPE cells take up both adenovirus[42,43] and adeno-associated virus[44], allowing the possibility of rescue experiments. As a therapeutic strategy, RPE transplantation is easier than that of photoreceptors, and in addition, the ultimate biochemical outcome of *Rpe65* deficiency, lack of 11-*cis* retinoids, may be amenable to pharmacological intervention.

Blockage of the metabolism of all-*trans*-retinyl ester to 11-*cis*-retinol underlies the *Rpe65*$^{-/-}$ phenotype, indicating that RPE65 may be the effector enzyme in the isomerization step yielding 11-*cis*-retinol. Alternatively, RPE65 may be involved in a previously unknown step required for isomerization. RPE65 is an obligate component of the isomerization reaction, essential to both vision and the visual cycle. Continued function of cones in the *Rpe65*-deficient mouse, however, provides new insight into cone pigment regeneration.

Methods

Generation of *Rpe65*-disrupted mice and genotype analysis. A P1 clone containing the entire mouse *Rpe65* was isolated from a 129SV mouse genomic library (Genome Systems). From this, a 7.7-kb *Eco*RI fragment containing exons 1, 2 and 3, and 2.8 kb of 5′ flanking region, was subcloned into Bluescript II SK (-) (T.M.R., unpublished data). A 1.7-kb *Eco*RI/*Afl*II fragment from the 5′ flanking region was subcloned into pLPG9 and linearized as an *Eco*RI/*Bam*HI fragment. A downstream 2.2-kb *Ecl*136II/*Eco*RI fragment from intron c was inserted into pLPG9 and linearized as an *Xho*I/*Not*I fragment. These linearized segments were inserted into X-pPNT to generate pPNT-Rpe65. pPNT-Rpe65 was linearized with *Not*I and electroporated into R1 ES cells[45]. Two ES clones with a targeted disruption were identified out of 31 clones isolated by the positive-negative G418/gancyclovir selection method. Targeted clones were identified by Southern-blot analysis after *Hin*dIII digestion of genomic DNA, using a flanking probe 3′ to the replacement. The wild-type allele was 4.9 kb, the targeted allele 5.9 kb. Clone ES-29 was microinjected into C57Bl/6 blastocysts and five chimaeric mice were produced. These chimaeras were bred with C57Bl/6 mice to generate progeny heterozygous for the mutation. Heterozygous mice were crossed to produce *Rpe65*$^{+/+}$, *Rpe65*$^{+/-}$ and *Rpe65*$^{-/-}$ mice. Germline transmission of the mutation was determined by Southern-blot analysis of tail DNA, as described above. All animal experiments were carried out under protocols approved by institutional Animal Care and Use Committees and followed the NIH "Using Animals in Intramural Research" guidelines.

***Rpe65* mRNA Assay**. Total RNA was isolated from whole mouse eyes using an RNeasy kit (Qiagen) and reverse transcribed using Moloney mouse leukaemia virus reverse transcriptase (Retroscript, Ambion). cDNA was PCR-amplified using mouse *Rpe65* exon 4 forward primer (5′–ATGATCGAGAAGAGGATTGTC–3′) and exon 6 reverse primer (5′–CTGCTTTCAGTGGAGGGATC–3′. Primers specific for mouse *Gapd* mRNA were: forward (starting at nt 586), 5′–ACCACAGTCCATGCCATCAC–3′ and reverse (starting at nt 1037), 5′–TCCACCACCCTGTTGCTGTA–3′. Cycle conditions used were: hot start at 94 °C, followed by 35 cycles (94 °C, 30 s; 55 °C, 30 s; 72 °C, 30 s). Product sizes were 366 and 452 bp for *Rpe65* and *Gapd*, respectively.

Light and electron microscopy. Tissues for light and electron microscopy were processed as described[46]. Thin (0.5 μm) sections were cut with glass knives and stained with toluidine blue for light microscopy. Ultrathin sections were cut with a diamond knife and stained with uranium and lead salts for electron microscopy. For immunocytochemistry, mouse eyes were processed as previously described[46]. Ultrathin sections were incubated for 1 h on affinity-purified anti-bovine opsin polyclonal antibodies diluted in 0.1 M sodium phosphate buffer (pH 7.2), containing 1% bovine serum albumin (BSA-phosphate buffer). The grids with their sections were washed in buffer and floated for 1 h on 1 part 18 nm colloidal gold adsorbed to affinity-purified goat antirabbit IgG (Jackson ImmunoResearch) and 15 parts BSA-phosphate buffer. Tissue contrast was enhanced by floating the specimens on 5% aqueous uranyl acetate for 10 min and Sato's lead stain for 3 min.

Electroretinography. Before measuring, ERG mice were anaesthetized with a mixture of ketamine:xylazine:urethane, and pupils were dilated with phenylephrine and atropine. ERGs were recorded with a wick-Ag:AgCl electrode placed on the cornea, a subcutaneous hypodermic needle (30 gauge) on the head as reference electrode and a ground placed subcutaneously in the neck region, all fed to a Tektronix A39 preamplifier with the half-amplitude bandpass set at DC to 3 kHz and displayed on an oscilloscope, and also fed to a computer running a Biopac M100 signal averaging program. The stimulus light source was either a quartz halogen lamp bulb (maximum stimulus intensity=1.59×10^3 cd/m^2) or a PS22 Grass stroboscopic flash unit (maximum stimulus intensity=5.52×10^2 cd/m^2 set at 8 and 40 Hz). The filament of the halogen lamp bulb was focused in the plane of a Uniblitz shutter (Vincent Assoc.), and another lens focused the filament on the tip of one arm of a bifurcated, randomized fiber optic bundle. The Grass stroboscopic bulb was focused on the tip of the other arm. The common arm of the bundle was brought into the Faraday cage and the tip was placed 1–2 mm from the cornea. The stimulus intensity was measured with a photometer (UDT Instruments) with the detector placed at the position of the cornea. Neutral density (ND) filters were used to reduce the full-intensity stimulus. The stimulus intensity was increased in 0.5 log unit steps, and two responses were averaged at the lower stimulus intensities (ND=6.0–3.5). Only one response was recorded at the higher stimulus intensities (ND=3.0–0). For flicker testing, responses were recorded to 2.5, 5, 7.5,10, 15 and 20 flashes/s at increasing stimulus intensities.

Rhodopsin assay. All procedures were carried out under red lights. Mice were killed, their eyes removed and retinae dissected and stored at −70 °C until required. Retinae were homogenized in 0.5 ml of Tris-HCl (10 mM), EDTA buffer (1.0 mM, pH 7.5) containing PMSF (1.0 mM) and DNase (10 μg) by a series of syringe triturations using progressively smaller needle sizes. (18G, 20G, then 26G). Syringes and tubes were rinsed with an additional buffer (0.5 ml) and pooled with the homogenate. This was centrifuged at 88,200×*g* at r max for 15 min. For regeneration experiments, the pellet is first resuspended in PBS and a fivefold excess of 11-*cis*-retinal added (~4 nM), incubated for 1 h at 4 °C on a rotator, centrifuged as above and the recovered pellet resuspended in 5% BSA in PBS and incubated for 30 min on a rotator at 4 °C. The regenerated sample was centrifuged as above to recover the pellet. Otherwise, after a PBS wash, the pellet was resuspended in 100 μl of 1% dodecyl maltoside in PBS and solubilized overnight at 4 °C on a rotator. Unsolubilized material was then removed by centrifugation at 109,000×*g* at r max for 15 min. Supernatant was analysed by spectroscopy on the WPI SpectroPette microspectrophotometer (World Precision Instruments). A total of five spectra were summed for each sample (both dark and bleached). For the bleached spectrum, light exposure was limited to 30 s due to extremely small sample volume (60 nanoliters per mm light path length). Data were exported into Kaleidagraph for difference spectra calculations.

Western-blot analysis. The membrane fractions of single retinae were dissolved in 100 μl PBS/1% dodecyl maltoside. For anti-opsin immunoblot analysis, these extracts were diluted 1:40 and 1 μl aliquots were resolved with SDS-PAGE (8–16% acrylamide gel) along with COS-1 cell membrane extract (50 ng) and purified bovine rhodopsin (5 ng) and electrotransferred onto Hybond-ECL nitrocellulose membrane (Amersham; 25 V, 2 h). For anti-transducin α-subunit immunoblot analysis, aliquots (10 μl) of undiluted retina membrane fraction extracts were used. The membranes were blocked by incubation with 5% (w/v) BLOTTO/TBST (20 mM Tris-Cl, pH 7.6, 137 mM NaCl, 0.1% Tween 20) for 2 h, and incubated with anti-rhodopsin monoclonal antibody 1D4 (22.5 μg/ml in BLOTTO/TBST; ref. 47) or anti-transducin α-subunit (Calbiochem; 1:200 in BLOTTO/TBST) overnight at 4 °C. Membranes were washed three times (15 min each at 25 °C) with BLOTTO/TBST and incubated in secondary antibody (horseradish peroxidase-conjugated rabbit anti-mouse IgG (Amersham) diluted (1:10,000) in BLOTTO/TBST for anti-opsin, or horseradish peroxidase-conjugated goat anti-rabbit IgG (Amersham) diluted (1:2,000) in BLOTTO/TBST for anti-transducin α subunit) for 3 h at 25 °C. The membranes were washed four times in TBST followed by 1 min incubation in the ECL (Amersham) developer substrate. The membranes were drained, covered with SaranWrap and exposed to a Kodak X-Omat film.

Retinoid and retinyl ester HPLC. Retinyl esters were extracted with methanol/hexane from dark-adapted whole mouse eyes or dissected mouse eye tissue homogenized in phosphate buffer[17] (0.1 M, pH 7.0). Retinyl esters were separated on a Lichrosorb SI-60 normal phase HPLC column (Alltech) in an Applied Biosystems or Waters HPLC system, using hexane/dioxane[48] or hexane/methyl t-butyl ether[17] mobile phase elution with detection at 320 nm. Experimental data were compared with 11-*cis*-retinal and 11-*cis*-retinol (synthesized by RKC), all-*trans*-retinol and all-*trans*-retinyl palmitate (Sigma) standards run on the same column. Saponification was done by incubating the dried ester HPLC fractions with 0.06 N ethanolic KOH (1 ml) at 55 °C for 30 min in the dark (J.C. Saari, pers. comm.). A minor amount of isomerization (<3%) occurs with this method. Hexane extracts were analysed by HPLC as above using 11.2% ethyl acetate/2% dioxane/1.4% 1-octanol in hexane as mobile phase[49].

Acknowledgements

We acknowledge the technical support of M. Lloyd, M. Kvaas and A. Van Dyke. We wish to thank S. Gentleman and G. Nuckolls for critical reading of the manuscript and for valuable suggestions. This research was supported in part by NIH grants EY00331 (D.B.), EY00444 (D.B.), EY12231 (J.X.M.) and EY04939 (R.K.C.) and by the Foundation Fighting Blindness (UCLA and MUSC). D.B. is a Research to Prevent Blindness Senior Scientific Investigator and Dolly Green Professor of Ophthalmology at UCLA.

Received 27 July; accepted 30 October 1998.

1. Hamel, C.P. *et al.* A developmentally regulated microsomal protein specific for the pigment epithelium of vertebrate retina. *J. Neurosci. Res.* **34**, 414–425 (1993).
2. Wright, A.F. A searchlight through the fog. *Nature Genet.* **17**, 132–134 (1997).
3. Gu, S. *et al.* Mutations in *RPE65* cause autosomal recessive childhood-onset severe retinal dystrophy. *Nature Genet.* **17**, 194–197 (1997).
4. Marlhens, F. *et al.* Mutations in *RPE65* cause Leber's congenital amaurosis. *Nature Genet.* **17**, 139–141 (1997).
5. Morimura, H. *et al.* Mutations in the *RPE65* gene in patients with autosomal retinitis pigmentosa or Leber congenital amaurosis. *Proc. Natl Acad. Sci. USA* **95**, 3088–3093 (1998).
6. Hamel, C.P., Jenkins, N.A., Gilbert, D.J., Copeland, N.G. & Redmond, T.M. The gene for the retinal pigment epithelium-specific protein RPE65 is localized to human 1p31 and mouse 3. *Genomics* **20**, 509–512 (1994).
7. Nicoletti, A. *et al.* Molecular characterization of the gene encoding an abundant protein specific to the retinal pigment epithelium. *Hum. Mol. Genet.* **4**, 641–649 (1995).
8. Hamel, C.P. *et al.* Molecular cloning and expression of RPE65, a novel retinal pigment epithelium-specific microsomal protein that is post-transcriptionally regulated *in vitro*. *J. Biol. Chem.* **268**, 15751–15757 (1993).
9. Båvik, C.-O., Lévy, F., Hellman, U., Wernstedt, C. & Eriksson, U. The retinal pigment epithelial membrane receptor for plasma retinol-binding protein. *J. Biol. Chem.* **268**, 20540–20546 (1993).
10. Simon, A., Hellman, U., Wernstedt, C. & Eriksson, U. The retinal pigment epithelial-specific 11-*cis* retinol dehydrogenase belongs to the family of short chain dehydrogenases *J. Biol. Chem.* **270**, 1107–1112 (1995).
11. Wald, G. Molecular basis of visual excitation. *Science* **162**, 230–239 (1968).
12. Saari, J.C. Retinoids in photosensitive systems. in *The Retinoids: Biology, Chemistry and Medicine* (eds Sporn, M.B., Roberts, A.B. & Goodman, D.S.) 351–385 (Raven, New York, 1994).
13. Bernstein, P.S., Law, W.C. & Rando, R.R. Biochemical characterization of the retinoid isomerase system of the eye. *J. Biol. Chem.* **262**, 16848–16857 (1987).
14. Winston, A. & Rando, R.R. Regulation of isomerohydrolase in the visual cycle. *Biochemistry* **37**, 2044–2050 (1998).
15. Barry, R.J., Canada, F.J. & Rando, R.R. Solubilization and partial purification of retinyl ester synthetase and retinoid isomerase from bovine ocular pigment epithelium. *J. Biol. Chem.* **264**, 9231–9238 (1989).
16. Peachey, N.S., Goto, Y., al-Ubaidi, M.R. & Naash, M.I. Properties of the mouse cone-mediated electroretinogram during light adaptation. *Neurosci. Lett.* **162**, 9–11 (1993).
17. Carter-Dawson, L. *et al.* Rhodopsin, 11-*cis* Vitamin A, and interstitial retinol-binding protein (IRBP) during retinal development in normal and rd mutant mice. *Dev. Biol.* **116**, 431–438 (1986).
18. Smeland, S. *et al.* Tissue distribution of the receptor for plasma retinol-binding protein. *Biochem. J.* **305**, 419–425 (1995).
19. Heller, J. & Bok, D. A specific receptor for retinol-binding protein as detected by the binding of human and bovine retinol-binding protein to pigment epithelial cells. *Am. J. Ophthalmol.* **81**, 93–97 (1976).
20. Sundaram, M., Sivaprasadarao, A., DeSousa, M.M. & Findlay, J.B.C. The transfer of retinol from serum retinol-binding protein to cellular retinol-binding protein is mediated by a membrane receptor. *J. Biol. Chem.* **273**, 3336–3342 (1998).
21. Wiggert, B., Bergsma, D.R., Lewis, M., Abe, T. & Chader, G.J. Vitamin A receptors. II. Characteristics of retinol binding in chick retina and pigment epithelium. *Biochim. Biophys. Acta* **498**, 366–374 (1977).
22. Noy, N. & Blaner, W.S. Interactions of retinol with binding proteins: Studies with rat cellular retinol-binding protein and rat retinol-binding protein. *Biochemistry* **30**, 6380–6386 (1991).
23. Robison, W.G. & Kuwabara, T. Vitamin A storage and peroxisomes in retinal pigment epithelium and liver. *Invest. Ophthalmol. Vis. Sci.* **16**, 1110–1117 (1977).
24. Young, R.W. & Bok, D. Autoradiographic studies on the metabolism of the retinal pigment epithelium. *Invest. Ophthalmol.* **9**, 524–536 (1970).
25. Travis, G. Insights from a lost visual pigment. *Nature Genet.* **15**, 115–117 (1997).
26. Lai, Y.L., Wiggert, B., Liu, Y.P. & Chader, G.J. Interphotoreceptor retinol-binding protein: possible transport vehicles between compartments of the retina. *Nature* **298**, 848–849 (1982).
27. Palczewski, K. *et al.* Rod outer segment retinol dehydrogenase: substrate specificity and role in phototransduction. *Biochemistry* **33**, 13741–13750 (1994).
28. Saari, J.C. & Bredberg, D.L. Lecithin: retinol acyl transferase in retinal pigment epithelial microsomes. *J. Biol. Chem.* **264**, 8636–8640 (1989).
29. Saari, J.C., Bredberg, D.L. & Noy, N. Control of substrate flow at a branch in the visual cycle. *Biochemistry* **33**, 3106–3112 (1994).
30. Maw, M.A. *et al.* Mutation of the gene encoding cellular retinaldehyde-binding protein in autosomal recessive retinitis pigmentosa. *Nature Genet.* **17**, 198–200 (1997).
31. Bridges, C.D.B. Distribution of retinol isomerase in vertebrate eyes and its emergence during retinal development. *Vision Res.* **29**, 1711–1717 (1989).
32. Humphries, M.M. *et al.* Retinopathy induced in mice by targeted disruption of the rhodopsin gene. *Nature Genet.* **15**, 216–219 (1997).
33. Liou, G.I. *et al.* Early onset photoreceptor abnormalities induced by targeted disruption of the interphotoreceptor retinoid-binding protein gene. *J. Neurosci.* **18**, 4511–4520, (1998).
34. Goldstein, E.B. Early receptor potential of the isolated frog (*Rana pipiens*) retina. *Vision Res.* **7**, 837–845 (1967).
35. Das, S.R., Bhardwaj, N., Kjeldbye, H. & Gouras, P. Muller cells of chicken retina synthesize 11-*cis*-retinol. *Biochem. J.* **285**, 907–913 (1992).
36. Jones, G.J., Crouch, R.K., Wiggert, B., Cornwall, M.C. & Chader, G.J. Retinoid requirements for recovery of sensitivity after visual-pigment bleaching in isolated photoreceptors. *Proc. Natl Acad. Sci. USA* **86**, 9606–9610 (1989).
37. Hood, D.C. & Hock, P.A. Recovery of cone receptor activity in the frog's isolated retina. *Vision Res.* **13**, 1943–1951 (1973).
38. Goldstein, E.B. & Wolf, B.M. Regeneration of the green-rod pigment in the isolated frog retina. *Vision Res.* **13**, 527–534 (1973).
39. Ma, J.-x, Xu, L., Lockman, D.K., Redmond, T.M. & Crouch, R.K. Cloning and localization of RPE65 mRNA in salamander cone photoreceptor cells. *Biochim. Biophys. Acta* (in press).
40. Chen, J. *et al.* The human blue opsin promoter directs transgene expression in short-wave cones and bipolar cells in the mouse retina. *Proc. Natl Acad. Sci. USA* **91**, 2611–2615 (1994).
41. Curcio, C.A., Sloan, K.R. Jr, Packer, O., Hendrickson, A.E. & Kalina, R.E. Distribution of cones in human and monkey retina: individual variability and radial asymmetry. *Science* **236**, 579–582 (1987).
42. Bennett, J., Wilson, J., Sun, D., Forbes, B. & Maguire, A. Adenovirus vector-mediated *in vivo* gene transfer into adult murine retina. *Invest. Ophthalmol. Vis. Sci.* **35**, 2535–2542 (1994).
43. Sullivan, D.M., Chung, D.C., Anglade, E., Nussenblatt, R.M. & Csaky, K.G. Adenovirus-mediated gene transfer of ornithine aminotransferase in cultured human retinal pigment epithelium. *Invest. Ophthalmol. Vis. Sci.* **37**, 766–774 (1996).
44. Ali, R.R. *et al.* Gene transfer into the mouse retina mediated by an adeno-associated viral vector. *Hum. Mol. Genet.* **5**, 591–594, (1996).
45. Nagy, A., Rossant, J., Nagy, R., Abramow-Newerly, W. & Roder, J.C. Derivation of completely cell culture-derived mice from early-passage embryonic stem cells. *Proc. Natl Acad. Sci. USA* **90**, 8424–8428 (1993).
46. Kedzierski, W., Lloyd, M., Birch, D.G., Bok, D. & Travis, G.H. Generation and analysis of transgenic mice expressing P216L-substituted rds/peripherin in rod photoreceptors. *Invest. Ophthalmol. Vis. Sci.* **38**, 498–509 (1997).
47. Molday, R.S. & MacKenzie, D. Monoclonal antibodies to rhodopsin: characterization, cross-reactivity, and application as structural probes. *Biochemistry* **22**, 653–660 (1983).
48. Bridges, C.D.B. & Alvarez, R.A. Measurement of the vitamin A cycle. *Methods Enzymol.* **81**, 463–485 (1982).
49. Landers, G.M. & Olson, J.A. Rapid, simultaneous determination of isomers of retinal, retinal oxime and retinol by high-performance liquid chromatography. *J. Chromatogr.* **438**, 383–392 (1988).